

Temporal evolution of different temperature plasma during explosive events

M. S. Madjarska and J. G. Doyle

Armagh Observatory, College Hill, Armagh BT61 9DG, N. Ireland

Abstract. High cadence observations (10 s exposure time) obtained with the SUMER spectrometer on-board SoHO in the Ly 6 (20 000 K) and S VI (200 000 K) lines reveal new insight on the nature of explosive events. A time delay in the response of the S VI line with respect to the Ly 6 line has been observed, with the Ly 6 line responding with about 20-40 seconds earlier. A temporal series obtained with 30 s exposure time and covering the entire Lyman series plus O I, C II and S VI (temperature range from 15 000 to 200 000 K) has also been explored showing the response of all these lines during transient phenomena. New common features linking explosive events and blinkers were found. During explosive events, the central intensity increases between 1.6 and 2.0 times the pre-event value while the same range of intensity increase was already reported during blinker phenomena. On the other hand the maximum intensity increase in Ly 6 was only 13 %.

Key words. Sun: SoHO–SUMER: Explosive events: Lyman lines

1. Introduction

Observations made with the Naval Research Laboratory's high resolution telescope and spectrograph (HRTS) revealed the existence of high velocity small-scale events seen in lines from ions formed at temperatures from $2 \cdot 10^4$ K (C II) to $2 \cdot 10^5$ K (N V) with no signature in chromospheric lines such as Si II ($1.3 \cdot 10^4$ K), C I ($6 - 10 \cdot 10^3$ K) and O I ($1.5 \cdot 10^4$ K), formed below $2 \cdot 10^4$ K (Brueckner & Bartoe 1983). Discovered and classified by Brueckner & Bartoe (1983) as turbulent events and jets, they are characterized by non-Gaussian profiles due to an enhancement in the blue and red wings, often observed with an offset along the slit (Dere *et al.* 1989; Innes *et al.* 1997a). Most of the events are predominantly blueshifted, showing velocities up to 250 km s^{-1} . Their first identification was followed by several studies based on observations obtained with HRTS and the spectrometer Solar Ultraviolet Measurements of Emitted Radiation (SUMER) on-board SoHO performed by Dere *et al.* (1989), Porter & Dere (1991), Innes *et al.* (1997a), Chae *et al.* (1998a), Pérez *et al.* (1999), Landi *et al.* (2000) and Teriaca *et al.* (2001). The authors extended the description of their general characteristics naming them by the term 'explosive events'.

The explosive events are located in the network lanes at the boundaries of the super-granulation cells where the neutral line separates regions of opposite magnetic polar-

ity (Dere *et al.*, 1991; Porter & Dere 1991). They appear preferably in regions with weak fluxes of mixed polarity or on the border of regions with large concentration of magnetic flux (Chae *et al.* 1998a). The average lifetime of the explosive events ranges from ~ 60 to 350 s (Dere 1994) with spatial dimensions of ~ 2500 km. They are often observed in bursts (Innes *et al.* 1997a) lasting up to 30 minutes in regions undergoing magnetic cancellation (Chae *et al.* 1998a). Using the density sensitive line intensity ratio O IV 1401.16/1404.81, Teriaca *et al.* (2001) found an electron density increase by a factor ~ 3 during explosive events. They also showed an increase of the line intensity ratio O IV 1401/O III 703 during an explosive event which suggests a temperature increase during the phenomena.

Explosive events seem to be a product of magnetic reconnection (Parker 1988; Porter & Dere 1991; Dere 1994; Innes *et al.* 1997b; Wilhelm *et al.* 1998; Roussev *et al.* 2001) because they tend to occur on the neutral line separating regions of opposite magnetic polarity, appear as bi-directional jets (Innes *et al.* 1997b) with velocities comparable to the local Alfvén velocity (Dere 1994), and they are often associated with a cancellation of photospheric magnetic flux (Dere *et al.* 1991; Dere 1994; Chae *et al.* 1998a).

After the launch of the SoHO satellite it became possible to observe Lyman lines with high spectral, spatial and temporal resolution. Using these lines as a plasma diagnostic tool has several advantages. They cover heights with a strong temperature gradient and therefore can be

used to diagnose the time evolution of different temperature structures. The cores of these optically thick lines are supposed to be formed in the chromosphere or at the base of the transition region while the wings are formed over large atmospheric depths in regions far below the core formation i.e. in the lower chromosphere (Vernazza *et al.* 1981). It was demonstrated by Heinzel *et al.* (1997) that the cores of the higher Lyman lines are sensitive to temperature because the upper levels of the corresponding transitions are strongly coupled to the kinetic temperature while the wings show sensitivity to the gas pressure. These lines are relatively strong and thus can be used for observations which need short exposures as in the case of explosive events. However, the observed profiles can only be interpreted correctly if multilevel NLTE (Non Local-Thermodynamic-Equilibrium) radiative transfer calculations are performed to explain the registered line shapes and intensities. That is why the present study is mainly based on the response of these lines during an explosive event through the emission changes in the blue and red wings of the registered lines.

Recently, Chae *et al.* (1998b), using SUMER data in Si IV 1402 Å and Big Bear Solar Observatory (BBSO) H α spectrograph observations, found that chromospheric upflow events rising in intranetwork areas are related to transition region explosive events. To support the idea of the chromospheric origin of some of the explosive events full spectrum observations covering lines with a wide range of formation temperature ($1.5 \cdot 10^4 - 2 \cdot 10^5$ K) have been analysed.

A new transient phenomenon observed with the Coronal Diagnostics Spectrometer (CDS) on-board SoHO as enhancements in the flux of transition region lines at network junctions was recently introduced by Harrison (1997) named as ‘blinkers’. Blinkers are mainly observed in lines of O III, O IV and O V while lines formed at lower and higher temperatures (such as He I and Mg X) show only a modest increase in intensity. They show a typical lifetime of ~ 17 minutes over an area of $\sim 5 \cdot 10^7$ km 2 , with an average intensity increase in O V of ~ 1.5 which, in extreme cases, can reach values as high as five times the pre-event level (Harrison *et al.* 1999). Chae *et al.* (2000) used CDS and SUMER coordinated observations in the transition region lines O V 629 Å (CDS) and Si IV 1402 Å (SUMER), and Big Bear Solar Observatory magnetograms to examine the relation between blinkers and explosive events showing similarities such as line profiles with enhanced wings, but on a different scale, suggesting the same physical origin of the two events, namely magnetic reconnection, but with different magnetic geometries.

This paper presents a study on the temporal evolution of a plasma with different temperatures during explosive events. In the next section we discuss the observations and the data reduction. § 3 presents the data analysis, paying attention on the line blends and event identification. The results are described in § 4 and the conclusions in § 5.

2. Observations and Data Reduction

In search of high cadence observations obtained in transition region lines, we selected a series of temporal observations from the SoHO archive performed with the SUMER spectrometer in S VI (933.38 Å) and Ly 6 (930.748 Å), and a full spectrum temporal series, covering all Lyman lines from Ly 4 up to the end of the series. The SUMER instrument is a high resolution stigmatic normal incidence spectrometer covering the wavelength range from ~ 400 to 1610 Å (Wilhelm *et al.* 1995; 1997; Lemaire *et al.* 1997) with a spatial resolution $\sim 1.5''$ and spectral pixels size between 42 mÅ and 45 mÅ. The datasets have been obtained on 1996 October 17 and 18 and 1997 June 5, pointing the instrument on the ‘quiet Sun’ at heliographic coordinates $X = 0''$ and $Y = 0''$ and $X = 696''.2$ and $Y = 158''.3$, respectively. In both cases the slit $1'' \times 120''$ was used.

The observations in 1996 (DS1) started on October 17 at 19:23:11 UT and finished on October 18 at 00:23:39 UT. The spectra were obtained exposing a band of 120 spatial \times 1024 spectral pixels (spectral range from 907 to 954 Å) on the central part of detector B for 200 s. A temporal sequence consisting of two spectral windows (120 spatial \times 50 spectral pixels) centered on Ly 6 930.748 Å and S VI 933.38 Å with 10 s exposure time was telemetered to the ground as well. No compensation for the solar rotation was applied and therefore for a solar rotation at this heliographic latitude of about $10''/1h$ the slit covered a region of $\sim 47''$.

The observations on 1997 June 5 (DS2) were obtained between 12:05:13 UT and 14:15:27 UT exposing for 30 s 120 spatial \times 1024 spectral pixels on detector B covering the wavelength range from 903 to 943 Å. This wavelength range includes the Lyman lines from Ly 5 up to the series limit, N IV, S VI and a few O I lines. In order to remain on the same position on the Sun a rotation compensation has been applied setting the tracking system to offset for the X -pointing by $0.75''$.

The reduction of SUMER raw images followed several stages such as local gain correction, flat-field subtraction and a correction for geometrical distortion. The signal to noise level is determined by the photon statistics.

Michelson Doppler Imager (MDI) (Scherrer *et al.* 1995) observations have been performed on 1996 October 17 and 18. The high resolution photospheric longitudinal magnetograms ($0.6''$ per pixel) were obtained with 60 s exposure time and field of view of 500×1024 pixels covering all the SUMER observing period. Magnetic cancellation during explosive events cannot be registered because of the high noise level (20 Gauss rms) of the MDI. Nevertheless these observations give a general picture of explosive events formation with respect to the solar magnetic network lanes and larger concentration of magnetic flux (Figure 1, right panel).

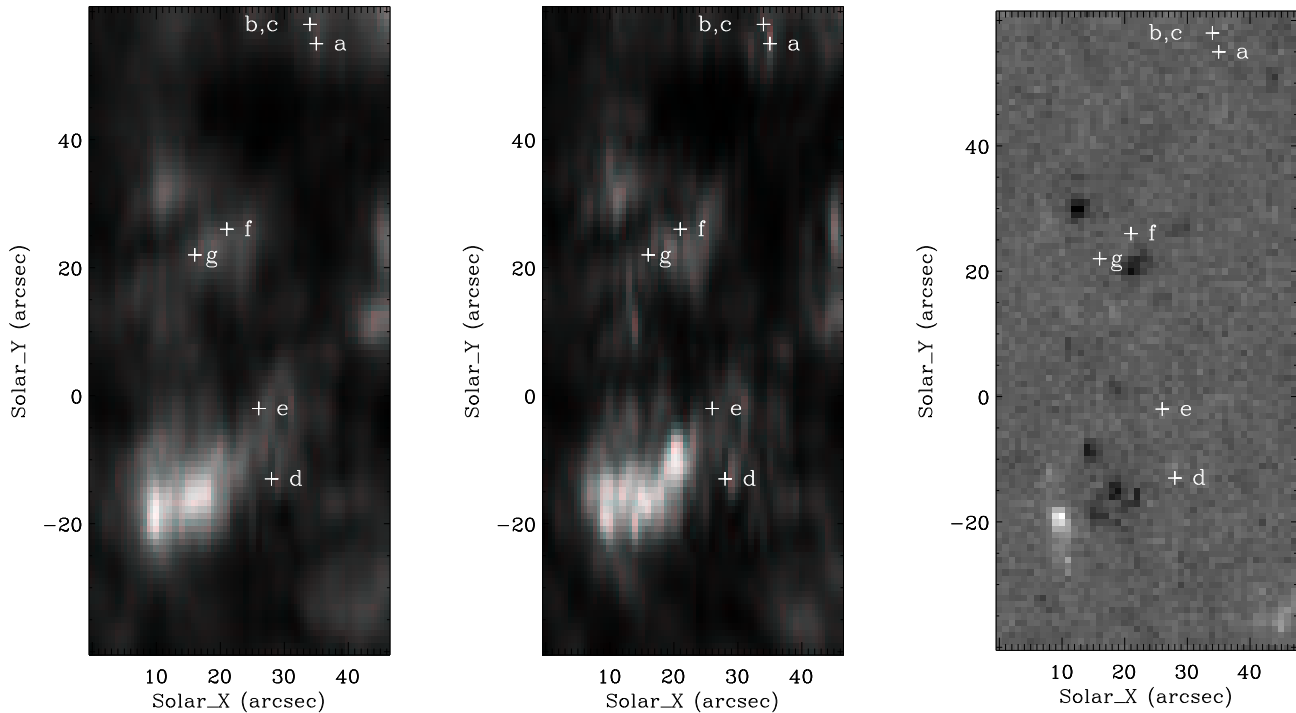


Fig. 1. Ly 6 (left) and S VI (middle) integrated line intensity images showing the network pattern and the locations of the explosive events marked by crosses and letters together with a MDI high resolution magnetogram (right) showing the position of explosive events with respect to magnetic flux concentrations. Note that the events ‘b’ and ‘c’ appear on the same position on the raster because we integrate over 390 seconds to reproduce each position of the slit on the Sun.

3. Data analysis

DS1 consists of a full spectrum obtained with 200 s integration time, prior to every 121 temporal spectra, covering the wavelength range from 907 to 954 Å. The spectra cover a few unblended O I lines such as O I 929.52 Å and O I 936.63 Å which have been used as a wavelength standard during the calibration. Since the reference lines are in general rather weak, we used profiles averaged along the slit to determine the centroids of these lines from a Gaussian fit. Both Ly 6 and S VI lines were registered during DS1 on the KBr part of the detector, and despite the short exposure time the signal-to-noise ratio is good. During DS2, however, the S VI line has been registered on the bare part, but the longer exposure still results in good photon statistics.

3.1. Line blends

Our study was based on the spectral lines listed in Table 1. In the present paper the Lyman lines (H I Ly #) will be written as Ly # for convenience, where # is the serial number of the line. Unfortunately, the lines belonging to the registered wavelength range are not free of contri-

bution from other emission lines, mainly He II ($T = 5.0 \cdot 10^4$ K) and/or O I ($T = 1.5 \cdot 10^4$ K) lines. Table 1 gives the blends as identified by Curdt *et al.* (1997, 2001) and Warren *et al.* (1998). The Ly 8 line is excluded from our analysis because it is blended by N IV lines which have a strong contribution in the very bright network and especially during explosive events.

The Ly 6 line is not effected by Ne VII 465.22 Å appearing in second order since the sensitivity of SUMER below 500 Å is very low. It is, however, blended by a first order O I 930.886 Å in the red wing, which could not be resolved. In the blue wing of Ly 6 are also O I 926.295 Å and He II 930.33 Å lines which appear as one feature and could be subtracted. These lines have a small, insignificant contribution of less than 10% to the blue wing of Ly 6 (Marsh *et al.* 1999). Our analysis is performed in a way (described in §3.2) ensuring that these blends do not influence the resulting response of the wings during explosive events. The other Lyman lines have small blends which do not effect our analysis and subsequent conclusions.

The S VI line at 933.38 Å is blended in the red wing by He II Balmer 12 at 933.44 (Curdt *et al.* 1997, 2001). The blend effect is variable, ranging between 10 and 20 % (W.

Table 1. The analysed lines and their corresponding blends.

Lines	λ (Å)	Blend
Ly 11	918.129	He II 917.74
Ly 10	919.35	O I 919.65
Ly 9	920.963	He II 920.62
Ly 7	926.84	He II 925.84
		O I 926.295
Ly 6	930.748	O I 926.295
		He II 930.33
		O I 930.886
S VI	933.378	Ne VII 465.22
		He II 933.44
O I	929.52	-
O I	936.63	-
C II	903.63	-
C II	903.96	-
C II	904.14	-
C II	904.48	-

Curdt, private communication). It can only be responsible for an overestimation of the count rate in the red wing of S VI. On the blue wing at 932.9 Å there is a faint unidentified line (W. Curdt, private communication) which has insignificant contribution to S VI. Both O I lines as well as the C II lines are clean from any blends.

3.2. Event identification

Whereas CDS blinkers have already been associated with small-scale short-lived SUMER ‘unit brightening events’ with a size of a few arc seconds and a lifetime of a few minutes (Chae *et al.* 2000, Teriaca *et al.* 2001) characterised by profiles with enhanced wings, explosive events show broader short- and longward shifted wings with velocities higher than 50 km s⁻¹. As will be shown later in this paper, the central line intensities, however, show a strong intensity increase in explosive events just like in blinkers, which has been reported to increase by about a factor of two, depending on the emission line under consideration (Harrison *et al.* 1999). From the point of view of spatial relationship, blinkers are found in the center of the network junctions (Harrison *et al.* 1997, 1999; Chae *et al.* 2000; Teriaca *et al.* 2001) while the explosive events tend to appear on the border of the network junctions and the super-granulation cells. Besides the location, the two events have also different size and duration. That is why a precise identification through a visual inspection is needed to correctly select each single event.

We selected a few explosive events by visual inspection of both S VI and Ly 6 slit images in the DS1, using the above mentioned wings at velocities > 50 km s⁻¹ as a criterion.

As was mentioned above, the observations were performed without applying rotational compensation, so the slit pointing at $X = 0''$ and $Y = 0''$ during 5.05 hr of observations resulted in a drift raster scan with a width of about 47''. Figure 1 shows the reproduced rasters in both

Table 2. Time difference in the response of the blue and red wing of Ly 6 compared to the S VI line.

Event	Blue wing Time (s)	Red wing Time (s)
a	40±9	40±2
b	13±6	11±1
c	79±21	33±10
d	–	19±6
e	31±14	16±4
f	39±7	–
g	16±4	28±6

Ly 6 and S VI lines with the corresponding locations of the explosive events marked by crosses and letters. The network pattern is visible on both rasters, less clear in Ly 6 due to the optical thickness of the Lyman line. An MDI image is also presented on this figure showing the region covered by the SUMER slit.

The events have a dimension along the slit Solar_Y $\sim 4''$ -5'' appearing in the network lanes away from larger concentration of magnetic flux. At the observed heliographic latitude the 1'' slit needs about 390 s to move to the neighboring position on the Sun which makes it impossible to evaluate the Solar_X dimension of the events.

In order to follow the temporal evolution of the phenomena through the emission changes in both wings, the total emission in the wings was estimated as the line intensity over 0.17 Å wide intervals centered 0.22 Å away from the central position on the blue and red sides of the spectral line. In this way we avoid most of the contribution of the blends. In the case of the Ly 6 line, the blends He II 930.32 Å and O I 930.26 Å are observed as one feature at 0.44 Å from the center of Ly 6. This blend was evaluated to be only $\sim 3\%$. In order to evaluate the central intensity increase, the centroids of the lines have been determined by a Gaussian fit of the line profile averaged along the slit in absence of high velocity events. The central intensity is that obtained within 0.13 Å around the central position.

After the visual identification, the duration of a single explosive event was defined as the period of a strong increase of the integrated emission in one of the wings until its decay.

4. Results

The DS1 consists only of one Lyman line (Ly 6) and the S VI line, but this temporal series has the advantage of a high temporal resolution (10 s exposure time) and containing two lines which have one order of magnitude difference in formation temperature. These two facts permit us to determine whether Ly 6 shows a response to explosive events, and if it does, what is the line profile shape and what is the temporal evolution of a different temperature plasma during these transient events?

First the strongest event was analysed, because a response of the optically thick Lyman lines could only be identified when the event is so strong that its emission is

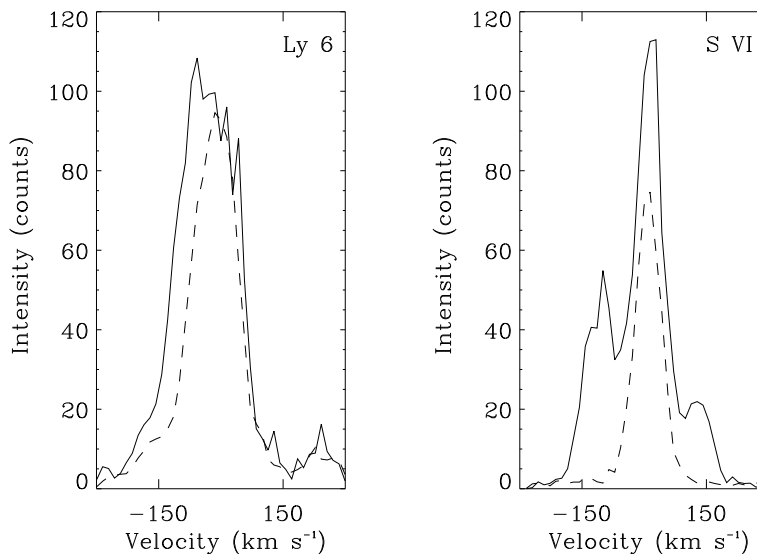


Fig. 2. Ly 6 and S VI profiles in explosive event ‘a’ during (solid line) and before the event (dashed line), obtained by binning over 7 pixels along the slit.

shifted far enough to be visible against the high background emission (Brueckner & Bartoe 1983). Figure 2 shows Ly 6 and S VI profiles during the event. We overplotted a pre-event profile in order to visualise the line shape and intensity changes. An increase in the blue wing in Ly 6 is clearly visible whereas the central intensity of the line does not show any significant change. The analysis of all line profiles showed that an increase in Ly 6 only becomes visible when at the same time the S VI central intensity increases by $\sim 100\%$ or more above the pre-event value.

All identified events were searched for a Lyman line response through the emission increase in the blue and red wings. In order to identify the start of a single event the background emission in the wing before or/and after the event was evaluated first. Note that the growth of the intensity in the wings for the two lines is different because of the different optical thickness of the Ly 6 and S VI lines. Through a visual inspection we determined the beginning of each event. It was defined as a point from the ascending branch of the intensity curve showing an obvious increase above the background emission. In order to improve the significance of the time delay measurements a few points above the starting one were also evaluated. Figure 3 presents the smoothed integrated intensity curves for all the registered events. The time differences for all events are given in Table 2. The time difference of the intensity peaks are easy distinguishable for events ‘a’, ‘b’, ‘c’, and ‘e’. The blue wing of event ‘d’ has a very complex behaviour and it is difficult to define its starting time. Events ‘f’ and ‘g’ already started before the observations begun (remember that a reference spectrum was obtained before each 121st spectrum). The time differences for these events are also given in Table 2, but have to be considered as lower limits. The general picture of the evolution

of all events is characterised by a blueshift accompanied by a redshift with the emission in the red wing often lower than in the blue one.

Concerning the intensity changes of the stationary component of the line we have determined a mean intensity increase in S VI of about 0.6 above the pre-event intensity. During the strongest one it reaches 0.9–1.0. However, only very small changes of the order of ~ 0.13 have been registered in Ly 6 due to the optical thickness of this line. Therefore, the observed self-absorption during the explosive events in Lyman lines may be mainly due to an emission increase in the wings. Figure 4 shows the intensity changes of the stationary component obtained in the way as described in §3.2. As was mentioned already, Harrison *et al.* (1999) have registered the same intensity increase of 0.2 - 0.3 above the pre-event value in the optically thick He I 584 Å and 1.0 in optically thin lines such as O V 629 Å, O III 599 Å and O IV 554 Å during blinker transient phenomena.

We defined the duration of a single event as the time from the intensity increase in the wing until its decay. Defined in that way, it was found that events with duration of more than 100 s show spikes in the wing intensity curve as was already observed by Dere *et al.* (1991). They are found to last between 40 and 100 s. Similar peaks, but on a different time scale, have also been observed during blinker events (Harrison *et al.* 1999). The authors suggested that this could be the result of the superimposed intrinsic solar variability.

The strong response of Ly 6 rises the question about the registration of the explosive events at lower temperature (below $2 \cdot 10^4$ K). To explore this idea we searched a full spectrum temporal series covering simultaneously Lyman lines ($< 20\,000$ K), O I ($\sim 15\,000$ K) lines and S VI ($\sim 200\,000$ K) line for explosive events. Only one

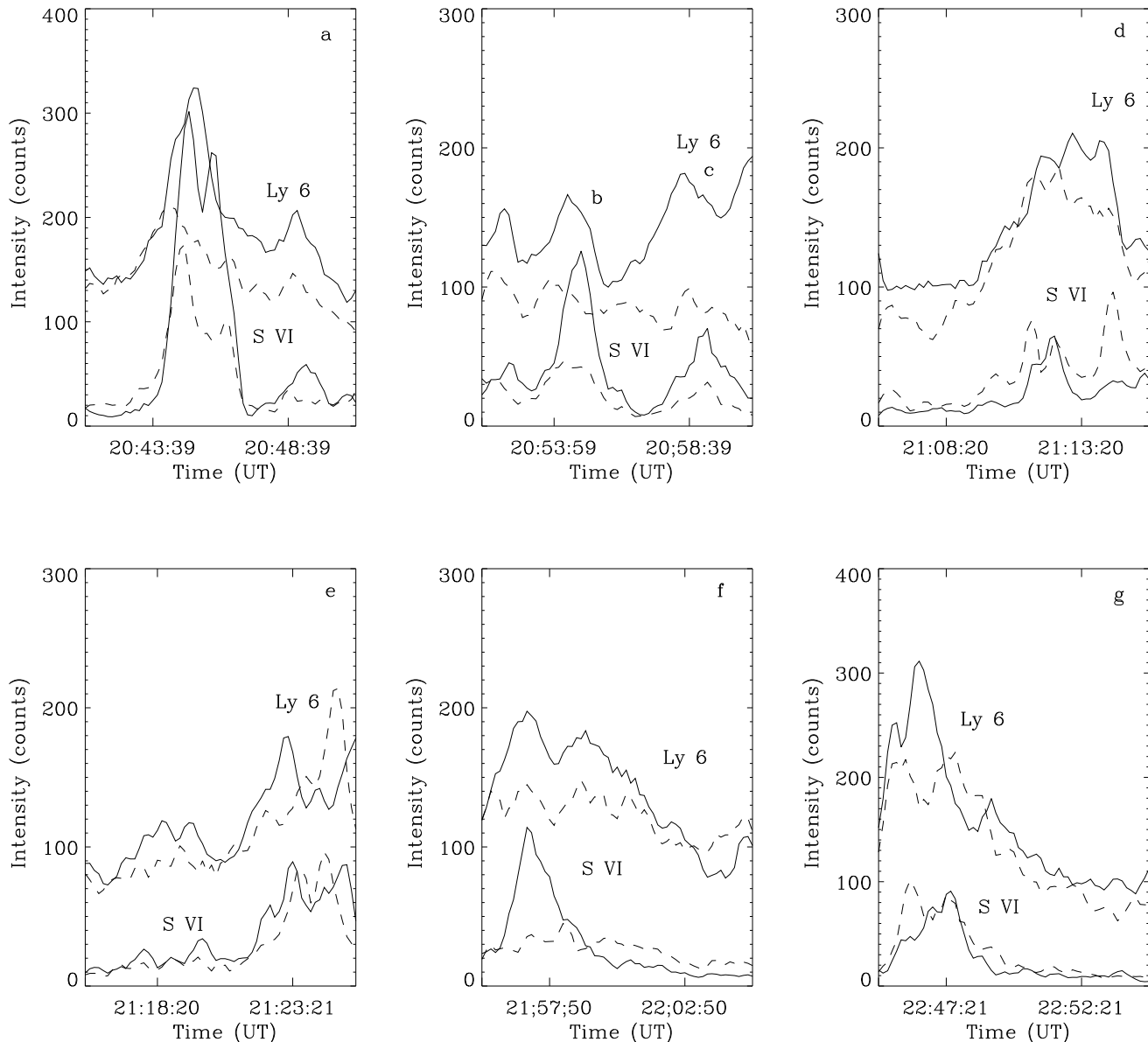


Fig. 3. Integrated intensity in the blue (solid line) and red (dashed line) wings of Ly 6 and S VI during the explosive events. The beginning of the events ‘f’ and ‘g’ are not registered because a reference spectrum was obtained before each temporal series.

event has been selected. Figure 5 displays the line profiles of the Ly 11 and S VI lines together with the corresponding slit negative images. The profiles were obtained by binning over 3 spectra and 5 pixels along the slit (note that S VI is registered on the bare part of detector B). The line profile before the explosive event does not show the presence of the faint feature at 932.9 Å and therefore we do not expect any significant contribution during the explosive event. Some of the Lyman lines show strong self-absorption, but as was mentioned above, this may be due to an increase of the emission in the wings as the central intensity slightly increases during the event.

Figure 6 shows the integrated intensity in the blue wings of Ly 11, Ly 10, Ly 9, Ly 7, Ly 6 and S VI obtained as described in §3.2. The total intensity of C II includes the intensity of four blended C II lines at 903.59, 903.99, 904.14, 904.46 Å (Curdt et al. 1997, 2001). We were especially interested in the response of the O I (15 000 K) lines. The visual inspection of these lines suggested some intensity increase during the explosive event, but this is uncertain because of the low emission of these lines. Therefore we used the total intensity in the two selected unblended oxygen lines O I 929.52 and 936.63 Å. As was shown above, the central intensity of optically thin lines increases by at least 1.6 and in optically thick lines by less than 1.2 times

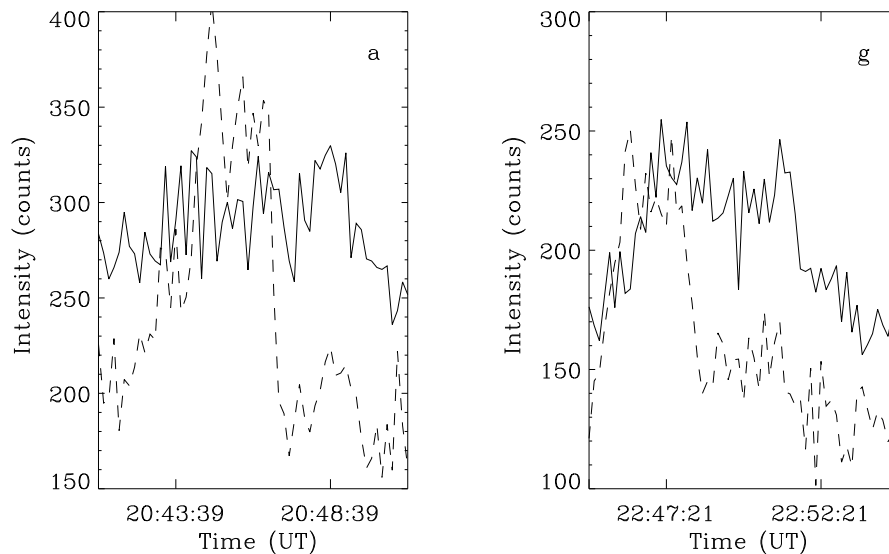


Fig. 4. Two examples of the stationary component intensity changes of the Ly 6 (solid line) and S VI (dashed line) lines during explosive events ‘a’ and ‘g’.

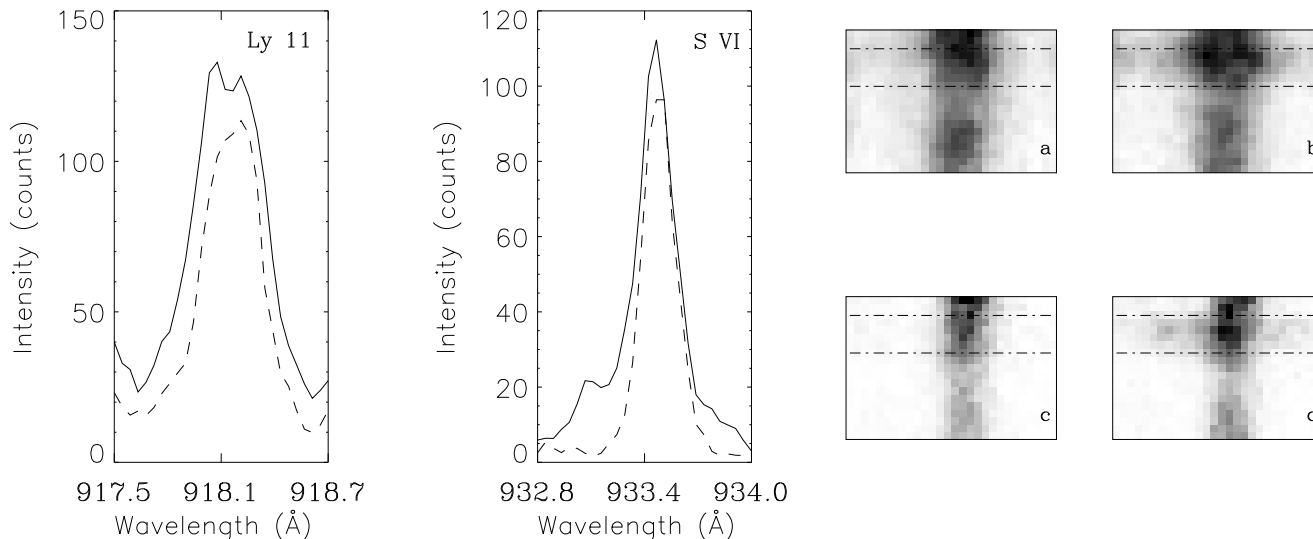


Fig. 5. Ly 11 and S VI line profiles before (dashed line) and during (solid line) the explosive event. The profiles are obtained by binning over 3 spectra and over the region along the slit as shown by the horizontal lines on the right panel slit negative images. *Right panels:* Slit negative images before and during the explosive event in Ly 11 (a, b) and S VI (c, d), respectively.

during an explosive event. Therefore, when it is impossible to detect blueshifted and redshifted emission as in the case of faint lines such as oxygen, and the event is already registered by other simultaneously recorded lines, the total intensity in these lines is a good indicator for the presence of the event in this spectral line. As can be seen from Figure 5, the continuum also shows an increase during the explosive event, which made it necessary to evaluate and subtract the background for each line. This is especially important in the case of the faint oxygen lines. The plots in Figure 6 show that during the event, a plasma with

a temperature from 15 000 to 200 000 K is registered. Unfortunately, the longer exposure time during these observations does not permit us to follow the temporal evolution of the different temperature plasma.

5. Conclusions

During the last decades numerous solar activity phenomena (solar flares, surges, sprays etc.) have been considered as manifestation of magnetic reconnection processes (Giovanelli 1946; Gold & Hoyle 1960; Priest 1981; Parker 1988; Forbes 1991, Priest & Forbes 2000) resulting from

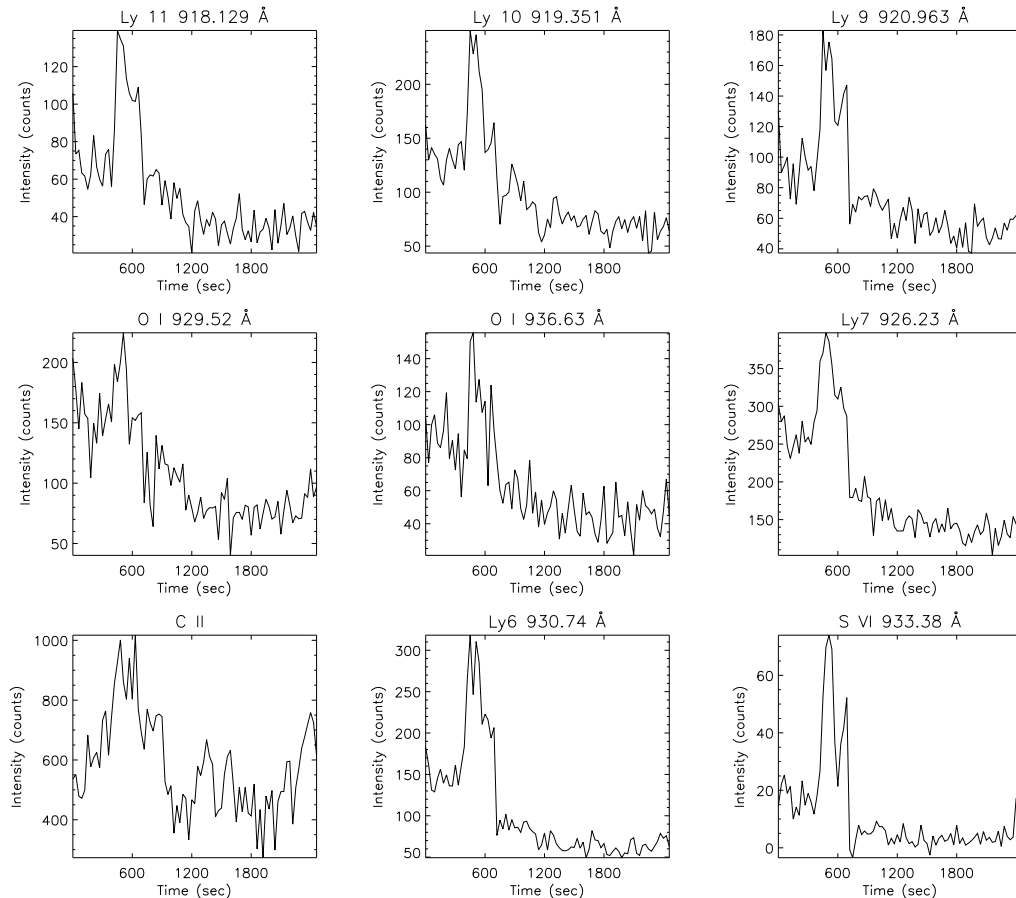


Fig. 6. Integrated intensity in the blue wing of Ly 11, Ly 10, Ly 9, Ly 7, Ly 6 and S VI in the region of the explosive event (5 pixels along the slit) for the all analysed dataset. We also show the total intensity of the O I and C II (includes four blended C II lines) lines .

the formation of a current sheet formed by magnetic flux tubes with opposite polarities pushed together by intensive photospheric motions. Such a current sheet may also occur between a new emerging flux tube and a pre-existing one. It is believed that the explosive events appearing as bi-directional jets with velocities comparable to the local Alfvén velocity are such events resulting from magnetic reconnection. This belief is due to their appearance on the super-granulation cell boundaries and the fact that they are often associated with the cancellation of the photospheric magnetic field.

Every explosive event shows some particularities and it is not possible to define a general picture of their behaviour. Two datasets complementing each other have been explored in this study trying to identify new common features for all of the events. We have examined the temporal evolution of different temperature plasmas during explosive events taking the advantage of having registered these phenomena with a short exposure time (10 s) in lines with one magnitude difference in the formation temperature. Another temporal series but covering simultaneously lines with a wide range of formation temperatures has been used to find out which temperature plasma is involved in this phenomenon. Our analysis revealed that

the explosive events appear first at chromospheric temperatures. After some time delay which differs from event to event a hotter plasma is registered.

Solar flares are another solar activity phenomena, resulting from magnetic reconnection. During their impulsive phase they are also registered in many EUV spectral lines ranging from neutral hydrogen and oxygen to highly ionised ions of metals (Priest 1981 and the citations therein). Results, with quite large uncertainties, from OSO-III observations (Hall 1971) suggest that probably similar time delays in the response of EUV emission lines exist during solar flares as well. The similarities between explosive events and flares suggest a common mechanism of their generation. This may help to find out why a plasma exists at such a wide temperature range during explosive events although not necessarily at coronal temperatures and how that is related to their generation.

Our study has been based on only a few events. In order to define the time evolution of plasma with different temperatures during explosive events further spectroscopic observations simultaneously covering lines with a wide range of formation temperatures obtained with high temporal resolution (exposure time around 10 s) are needed. Koutchmy *et al.* (1997) provided evidence for the

existence of a new type of soft X-ray brightening event with duration and size comparable to the explosive events and called them ‘soft X-ray coronal flashes’. To find out whether these phenomena are the coronal counterpart of the explosive events simultaneous multi-instrumental and spectroscopic multi-wavelength observations have to be obtained.

Such observations are also needed to explore the connection and similarities between explosive events and blinkers. Chae *et al.* (1998) using SUMER and CDS observations have already revealed some similarities between explosive events and blinkers. CDS blinkers have been associated with small-scale short-lived SUMER ‘unit brightening events’ with a size of a few arc seconds and a lifetime of a few minutes (Chae *et al.* 2000, Teriaca *et al.* 2001) characterised by profiles that are not as broad as those of explosive events but still with significantly enhanced wings. In this work two more common features of the two events have been identified. We compared the intensity increase of the ‘line at rest’ during explosive events and blinkers (reported by Harrison *et al.* 1999) and found out that the same intensity increase takes place during both events. The existence of intensity peaks during an explosive event, registered also with HRTS by Dere *et al.* (1989), is another link between explosive events and blinkers.

Further efforts are required regarding time delays of the response of different spectral lines during explosive events as well as a more detailed NLTE study concerning the line formation of optically thick lines such as the Lyman series. The present observational dataset suggests a time delay with the chromospheric feature being detected first as a blueshifted plasma several seconds before a response to the magnetic reconnection is observed at transition region temperatures.

Acknowledgements. Research at Armagh Observatory is grant-aided by the N. Ireland Dept. of Culture, Arts and Leisure, while partial support for software and hardware is provided by the STARLINK Project which is funded by the UK PPARC. This work was supported by PPARC grant PPA/GIS/1999/00055. The SUMER project is financially supported by DLR, CNES, NASA, and PRODEX. Thanks to Prof. E. Priest and Dr. W. Curdt for fruitful discussions.

References

- Brueckner, G.E. & Bartoe, J.-D.F., 1983, *ApJ*, 272, 329
 Chae, J., Wang, H., Lee, C.Y., Goode, P.R. & Schühle, U., 1998a, *ApJ*, 497, L109
 Chae, J., Wang, H., Lee, C.Y., Goode, P.R. & Schühle, U., 1998b, *ApJ*, 504, L123
 Curdt, W., Feldman, U., Laming, J.M., Wilhelm, K., Schühle, U., & Lemaire, P., 1997, *A&AS*, 126, 281
 Curdt, W., Brekke, P., Feldman, U., Wilhelm, K., Dwidel, B. N., Schühle & Lemaire, P., 2001, *A&A*, 375, 591
 Dere, K.P., Bartoe, J.-D.F. & Brueckner, G.E., 1989, *Solar Phys.*, 123, 41
 Dere, K.P., Bartoe, J.-D., Brueckner, G.E., Ewing, J. & Lund, P., 1991, *J. Geophys. Res.*, 96, 9399
 Dere, K.P., 1994, *Adv. Space Res.*, 14(4), 13
 Forbes, T.G., 1991, *Geophys. Astrophys. Fluid Dyn.*, 62, 15
 Giovanelli, R.G., 1946, *Nature*, 158, 81
 Gold, T. & Hoyle, F., 1960, *MNRAS*, 120, 89
 Hall, L.A., 1972, *Solar Phys.*, 21, 1971
 Harrison, R.A., Sawyer, E.C., Carter, A.M. et al., 1995, *Solar Phys.*, 162, 233
 Harrison, R.A., 1997, *Solar Phys.*, 175, 467
 Harrison, R.A., Fludra, A. & Pike C.D., et al., 1997, *Solar Phys.*, 170, 123
 Harrison, R.A., Lang, J., Brooks, D.H. & Innes, D. E., 1999, *A&A*, 351, 1115
 Heinzel, P., Schmieder, B. & Vial, J.-C., 1997, *Proc. Fifth SoHO Workshop (ESA SP-404)*; Nordwijk: ESA, 427
 Innes, D.E., Brekke, P., Germerott, D. & Wilhelm, K., 1997a, *Solar Phys.*, 175, 341
 Innes, D.E., Inhester, B., Axford, W.I. & Wilhelm, K., 1997b, *Nature*, 386, 811
 Koutchmy, S., Harra, H., Suematsu, Y. & Reardon, K., 1997, *A&A*, 320, 33
 Lemaire, P., Wilhelm, K., Curdt, W. et al., 1997, *Solar Phys.*, 170, 105
 Marsh, E., Tu, C.-Y., Heinzel, P., Wilhelm, K. & Curdt, W., 1999, 347, 676
 Parker, E.N., 1988, *ApJ*, 330, 474
 Pérez, M.E., Doyle, J.G., Erdélyi, R. & Sarro, L.M., 1999a, *A&A*, 342, 279
 Porter, J.G. & Dere, K. P., 1991, *ApJ*, 370, 775
 Priest, E.R., 1981, *Solar Flare Magnetohydrodynamics*, Gordon & Breach, London
 Priest, E.R. & Forbes, T., 2000, *Magnetic Reconnection: MHD theory and applications*, Cambridge Univ. Press
 Roussev, I., Galsgaard, K., Erdélyi, R. & Doyle, J.G., 2000, *A&A*, 370, 298
 Sherrer, P.H., et al. 1995, *Sol. Phys.*, 162, 129
 Teriaca, L., Madjarska, M. S. & Doyle, J.G., 2001, *Solar Phys.*, 200, 91
 Vernazza, J.E., Avrett, E. H. & Loeser, R., 1981, *ApJS*, 45, 635
 Warren, H. P., Mariska, J. T. & Wilhelm, K., 1998, *ApJS*, 119, 105
 Wilhelm, K., Curdt, W., Marsch, E., Schühle, U., Lemaire, P., Gabriel, A., Vial, J.-C., Grewing, M., Huber, M.C.E., Jordan, S.D., Poland, A.I., Thomas, R.J., Kühne, M., Timothy, J.G., Hassler, D.M. & Siegmund, O.H.W., 1995, *Solar Phys.* 162, 189
 Wilhelm, K., Lemaire, P., Curdt, W. et al., 1997, *Solar Phys.*, 170, 75
 Wilhelm, K., Innes, D.E., Curdt, W., Kliem, B. & Brekke, P., 1998, in *Solar Jets and Coronal Plumes*, Guadalupe, France, ESA-SP 421, 103